Fault detection Technique for High Voltage Power Transformers

George M. Sobhy, Ali M. El-Rifaie, R.M. Sharkawy

***Abstract*— This paper proposes a new technique for fault detection in high voltage power transformers. The technique relies on measuring the features of voltage versus current images obtained at both sides of the transformer. The images obtained on both sides of the transformer will have an elliptical shape, whose width, direction and center relies on the loading conditions of the transformer. During normal operation, the two ellipses are having two centers almost equal to zero. However, during internal and external faults, the elliptical shape will be distorted and centers will effectively change. The proposed algorithm is detecting the change in both magnitude and direction of the images centers to detect faults and discriminate between internal and external ones. The proposed technique is applied on a simulated model obtained by ATP. The simulated transformer is 132/11 kV 155 MVA double fed transformer. Internal faults covering different percentages of the transformer windings were introduced. The obtained simulation results, obtained using MATLAB, showed the ability of the proposed technique to detect fault presence and discriminate between internal and external faults for all fault types.**

Index Terms—Power transformer, Ellipse Technique, High Voltage Networks, Digital Protection.

I. Introduction

Power Transformer play an essential role in modern power systems, which is basically connecting different voltage levels of different zones. Although disconnecting loads due to faults can affect the stability and reliability of the system; however, a non-detected fault will lead to permanent loss of the transformer in addition to power interruption. Transformers in HV networks are always protected by main protection device however, back-up protection device should be considered [1]. Protective devices are used with different protection schemes to provide safe and secure power to the customers and to maintain the reliability of the system. The operation of the protective scheme for power transformer is limited to internal faults, and it must not be triggered by any fault outside the protection zone. Differential protection, overcurrent protection, ground fault protection and overvoltage protection are the main types of electrical protection provided to HV transformers [2]. Differential protection is the most common protection scheme used. However, there has always been attempts to improve the current protection scheme by using digital relays [3]. Ivo Brncic [4] proposed a discriminating technique between internal and external faults using negative sequence differential current. However, the internal-external fault discriminator needs the transformer to be connected to a load.

George M. Sobhy: Electrical & Control Engineering Dept., College of Engineering AASTMT, Cairo, Egypt george.michel.s@hotmail.com
Ali M. El-Rifaie (SMIEEE): College of Engineering and Technology, American University of the Middle East, Kuwait ali.el-rifaie@aum.edu.kw
R.M. Sharkawy: Electrical & Control Engineering Dept., College of Engineering AASTMT, Cairo, Egypt rania.m.elsharkawy@aast.edu

This can avoid false tripping due to initial magnetizing current inrush. Manoj Tripathy [5] suggested using a hybrid system of power differential protection with a Probabilistic Neural Network to discriminate between internal faults and inrush current at power transformer. Rupanjali Umre [6] proposed using Clark's transformation to pre-process the signal while using fuzzy logic to define the fault type. Masoud Ahmadipour [7] used slatlet transform to extract features from the wave form and two artificial neural networks to detect the fault and its type. Wavelet transform-based techniques have been proposed for fault detection and discrimination. One of the techniques compared the variation of the last samples using discrete wavelet transform with a predefined threshold value [8]. Meanwhile another technique used Artificial neural network over wavelet transform to improve the fault discrimination [9]. The improved Prony's algorithm was used to improve the differential relay performance through obtaining the power frequency fault current based on unsaturated short data window [10] . In this paper a technique for fault detection and discrimination in HV transformers is proposed, the technique was previously introduced and known as the Ellipse Technique (ET). The ET was applied on EHV transmission networks as well as EHV bus bars [11-14] and succeeded in detecting, discriminating all fault cases besides determining fault types within a total time of 20 msec. (F=50 Hz).

II. The Proposed technique

The ET produces an image describing the instantaneous current versus the instantaneous voltage signals plot [9-11]; the produced image has a uniform elliptical shape during normal operating conditions and has irregular shapes during fault ones. A simulation study is done using ATP [15]. Figure 1 shows the simulated network. The network data are provided in Table I.

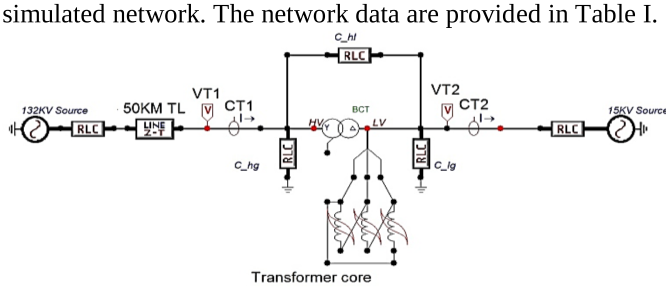

Fig. 1. Simulated network using ATP

TABLE I. DATA OF THE SIMULATED NETWORK

Equipment	Data
Generator (1)	132 kV
Generator (2)	15 kV
Transformer	155MVA-132kV/15kV
Transmission Line	50 Km - 500Ω impedance

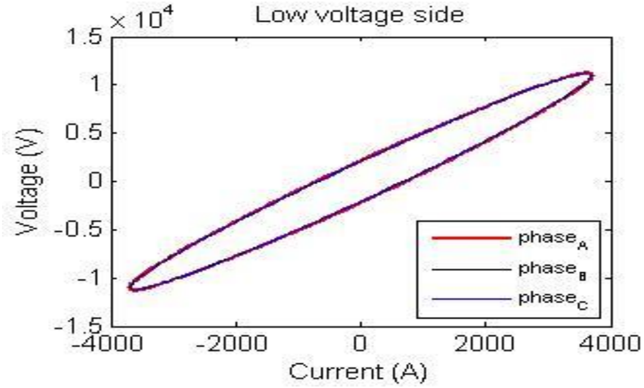

Fig. 2. Three Phase Ellipses at Transformer High Voltage Side

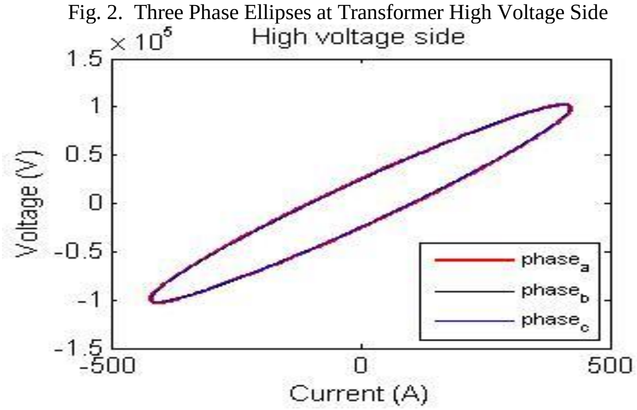

Fig. 3. Three Phase Ellipses at Transformer Low Voltage Side

Fig. (2) and Fig. (3) show the three phase ellipses of the transformer high voltage side and low voltage side respectively during normal operation conditions. The uniform elliptical shape has several features [14], one of which is being uniform with the same shape as long as the system is operating normally, another is its horizontal-vertical boundaries. The center value is a fixed feature that is not affected by load value or power flow direction, it will have an approximate value of zero during normal operation. This value will also decrease after normalizing the ellipse shape by dividing the voltage signal over its peak value, and the current signal over the peak value of the maximum short circuit current of the power transformer as shown by equations 1-2 respectively [14]. After normalization of the current and voltage, the center will be calculated according to equations 3-5 respectively. Fig. (4) and Fig. (5) shows the new elliptical shapes after normalization, while Table II shows the normalized calculated values of the ellipses centers.

$$v_{n(i)} = \frac{v_{(i)}}{v_{peak}} \tag{1}$$

$$i_{n(i)} = \frac{i_{(i)}}{i_{sc\,max.}} \tag{2}$$

$$v_o = \sum_{i=1}^{N} v_{n(i)}/N \tag{3}$$

$$i_o = \sum_{i=1}^{N} i_{n(i)}/N \tag{4}$$

where N is the total number of samples in one complete cycle.

$$k_o = \sqrt{{v_o}^2 + {i_o}^2} \tag{5}$$

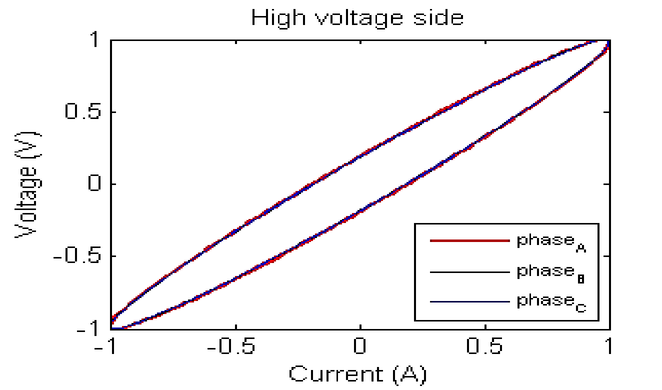

Fig. 4. Three Phase normalized Ellipses at Transformer High Voltage Side

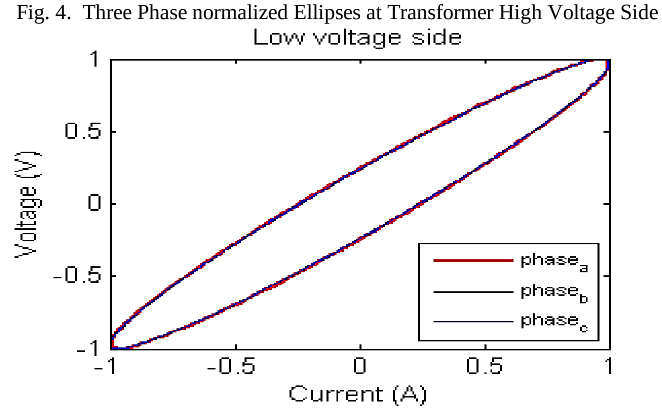

Fig. 5. Three Phase Normalized Ellipses at Transformer Low Voltage Side

TABLE II. NUMERICAL VALUES FOR THREE PHASE NORMALIZED CENTERS DURING NORMAL OPERATION FOR ONE COMPLETE CYCLE

	V_0	i_0	K_0
H.V Phase A	0.00000996	0.00007874	0.00007936
H.V Phase B	-0.00001109	-0.00001111	0.00001569
H.V Phase C	0.00000141	-0.00004454	0.00004456
L.V Phase A	0.00001075	0.00005166	0.00005277
L.V Phase B	-0.00000715	0.00000289	0.00000771
L.V Phase C	-0.00000684	-0.00005668	0.00005709

A. Updating the 2D Center

At normal condition of the transformer, after normalizing the current and the voltage signals. The values of each center is updated at every sample and compared with the previous cycle for the same interval as shown in equations 6-9 respectively [8]. The threshold value is obtained for the two voltage sides by collecting enough data at normal case and detecting the largest change in the center value.

$$v_{0(N+i)} = v_0 + (v_{n\,(N+i)} - v_{n\,(i)})/N \tag{6}$$

$$i_{0(N+i)} = i_0 + (i_{n\,(N+i)} - i_{n\,(i)})/N \tag{7}$$

$$k_{0(N+i)} = \sqrt{{v_{0(N+i)}}^2 + {i_{0(N+i)}}^2} \tag{8}$$

ISBN: 978-988-14048-6-2
ISSN: 2078-0958 (Print); ISSN: 2078-0966 (Online)

$$k_{0diff} = |k_{0\,(i)} - k_{0\,(i-1)}| \quad (9)$$

The value of k_{0diff} is updated each received sample for both sides of the transformer. The values of k_{0diff} for six complete cycles at both transformer sides during normal operation are shown in Tables III and IV respectively.

TABLE III. THE CHANGE IN ELLIPSE CENTERS AT HIGH VOLTAGE SIDE

Cycle number	k_{0diff} at Phase A	k_{0diff} at Phase B	k_{0diff} at Phase C
2	0.00001854	0.00003324	0.00002272
3	0.00002215	0.00002165	0.00000422
4	0.00002599	0.00000687	0.00001571
5	0.00001525	0.00001044	0.00001567
6	0.00002538	0.00003073	0.00000765

TABLE IV. THE CHANGE AT ELLIPSE CENTERS AT LOW VOLTAGE SIDE

Cycle number	k_{0diff} at Phase A	k_{0diff} at Phase B	k_{0diff} at Phase C
2	0.00003025	0.00001537	0.00000566
3	0.00001373	0.00001586	0.00001758
4	0.00003111	0.00000289	0.00002539
5	0.00005537	0.00000780	0.00002137
6	0.00005533	0.00000867	0.00000295

Simulation results showed that the value of k_{0diff} never exceeded 0.00005537. The threshold value is obtained by doubling the maximum value of k_{0diff} to ensure reliability. The threshold value of 0.00011074 is calculated through using a sampling frequency of 12.8 KHz (256 sample per cycle, F= 50 Hz); however, the value of k_{0diff} will change rapidly due to the presence of any abnormal conditions and that include both high load switching and fault occurrence.

B. Fault Detection Criterion

The Fault detection criteria is triggered when k_{0diff} of high voltage or low voltage side of the transformer exceed the threshold value. The readings of k_0 will be compared again with the k_0 during normal operation after one complete cycle from the instance of fault detection. the value of k_{0diff} will be compared for a second time with the threshold value to avoid mal-operation due to load switching and to confirm the fault occurrence.

C. Fault Discrimination

The values of $i_{n\,at\,H.V}$, $i_{n\,at\,L.V}$ are captured after the instance of fault detection by 16 sample (1/16 cycle) and compared with the $i_{n\,at\,H.V}$, $i_{n\,at\,L.V}$ of the previous cycle. This difference will be calculated for high voltage side as $\Delta i_{at\,H.V}$ and for the low voltage side as $\Delta i_{at\,L.V}$ as shown in equations 10-11.

$$\Delta i_{at\,H.V} = i_{(16)} - i_{(16-N)} \quad (10)$$

$$\Delta i_{at\,L.V} = i_{(16)} - i_{(16-N)} \quad (11)$$

$\Delta i_{at\,H.V}$ and $\Delta i_{at\,L.V}$ used for discrimination of fault type. In case of external fault it was noticed that the polarity of $\Delta i_{at\,H.V}$ and $\Delta i_{at\,L.V}$ are the same either positive or negative. However during internal fault the polarity of $\Delta i_{at\,H.V}$ and $\Delta i_{at\,L.V}$ are opposite where one side is positive and the other side is negative. The polarity is the same at external fault because the current on both sides of the transformer will be having the same direction feeding the external fault. However, during internal fault the current will be in opposite direction feeding the fault internally and sending signal to the relay. Fig. (6) and Fig. (7) shows the difference in ellipse shape during the first 16 samples (1/16 cycle) of an internal and Fig. (8) and Fig. (9) for external fault.

k_0 is calculated for 1 complete cycle in parallel with $\Delta i_{n\,at\,H.V}$ and $\Delta i_{n\,at\,L.V}$ after the fault detection criteria is triggered. k_0 is used to detect fault presence and discriminate it from normal and load switching condition. While $\Delta i_{n\,at\,H.V}$ and $\Delta i_{n\,at\,L.V}$ are used for discriminating internal faults from external ones as described by the flowchart shown in Fig. (10).

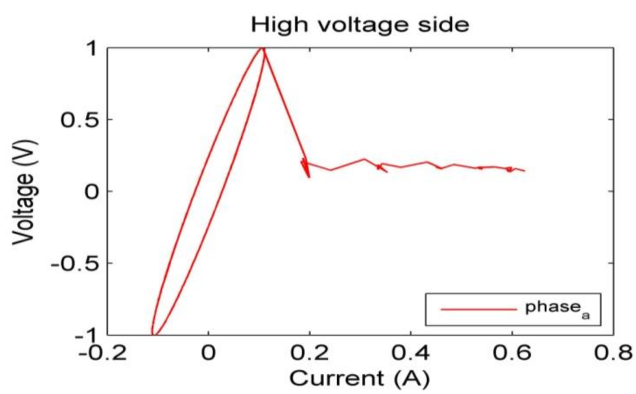

Fig. 6. Ellipse after 1/16 cycle of internal fault at 80% windings of high voltage side phase A.

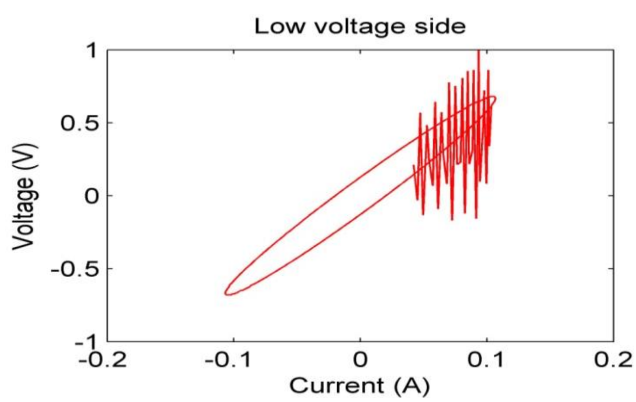

Fig. 7. Ellipse after 1/16 cycle of internal fault at 80% windings of low voltage side phase A.

ISBN: 978-988-14048-6-2
ISSN: 2078-0958 (Print); ISSN: 2078-0966 (Online)

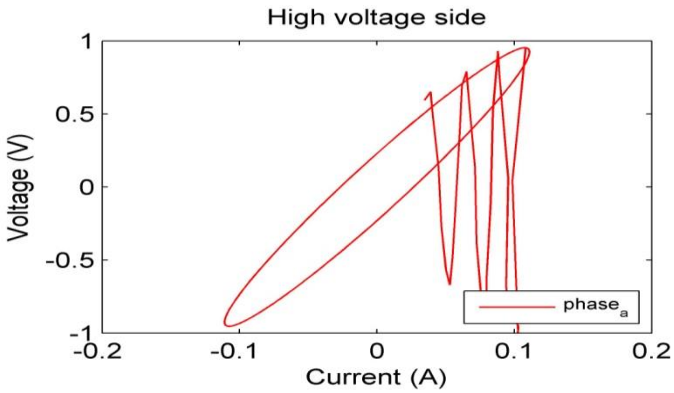

Fig. 8. Ellipse after 1/16 cycle of external fault at high voltage side phase A.

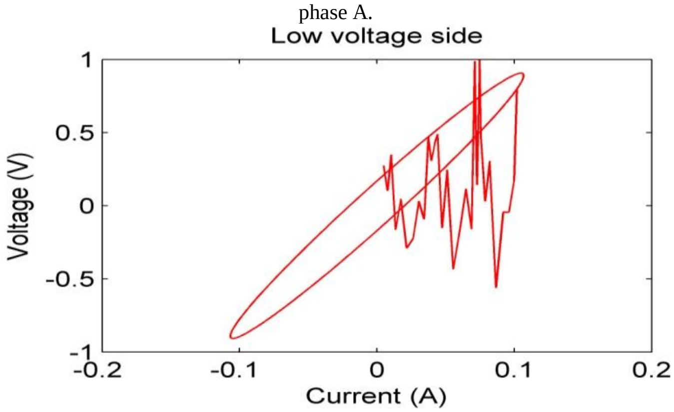

Fig. 9. Ellipse after 1/16 cycle of external fault at low voltage side phase A.

III. CASE STUDY

The ellipse technique was studied for different cases such as, normal operating case, phase to ground fault at different percentage of windings, fault at transformer bushing, external fault at difference distances. The model used to obtain these types of faults was implemented using Alternative Transient Program (ATP). The model consisted of a (155MV) power transformer mode of 132kV/15kV, two generators G1, G2 from the two sides of the transformer, RLC line impedance to simulate the external fault. ATP used to simulate normal case, internal fault and external fault data with a sampling rate of 12.8 kHz. This data is tested by Matlab application to verify fault detection and discrimination.

A. Normal Case

At normal operating conditions, The k_0 was calculated for both sides of the transformer. After one complete cycle the value of k_{0diff} was calculated and updated with each sample. The k_{0diff} highest values were 0.00005537 for low voltage side, 0.00003324 for high voltage side as shown at previous Table III and Table IV. The values are compared with the threshold value of 0.00011074. None of the values during the normal case condition at any side of the transformer exceeded the threshold value.

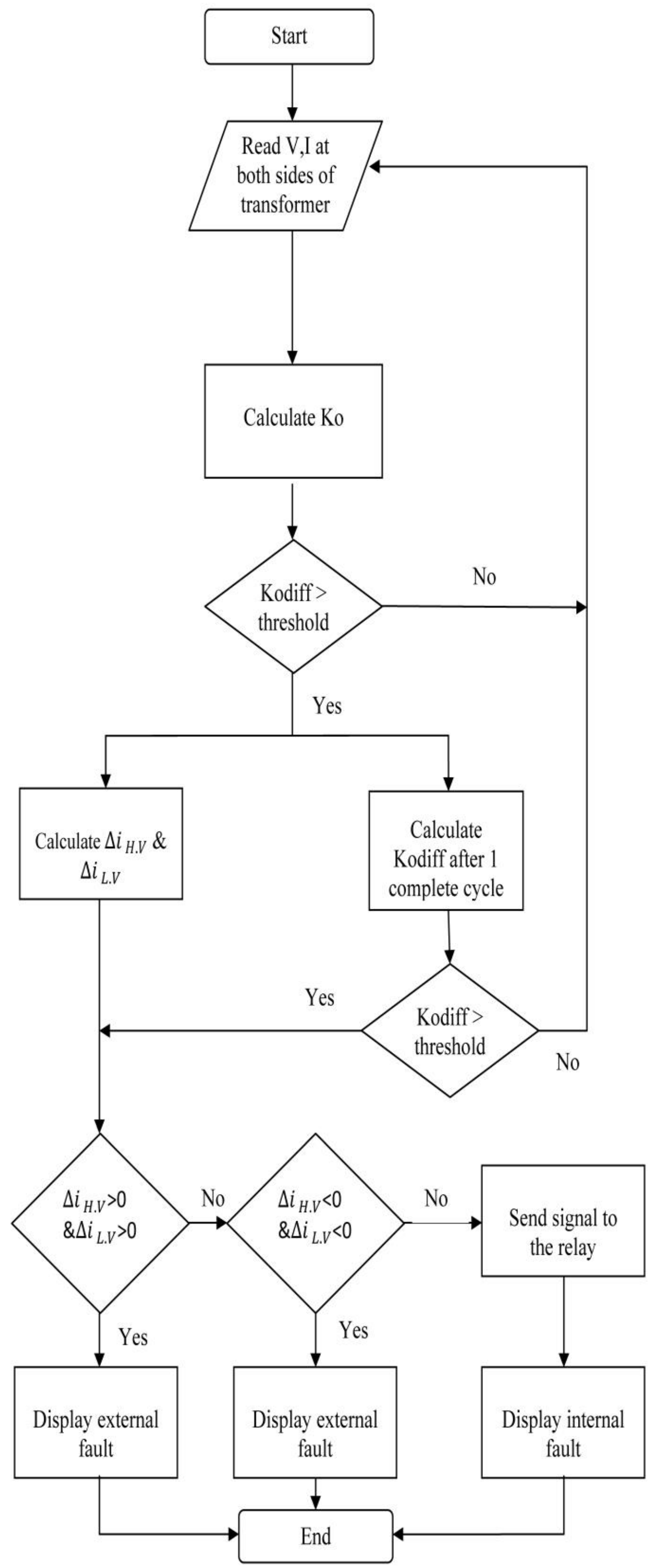

Fig. 10. Flowchart of fault detection and fault type discrimination

ISBN: 978-988-14048-6-2
ISSN: 2078-0958 (Print); ISSN: 2078-0966 (Online)

B. External Fault Case

Three cases of external fault were studied at different inception angles. The fault is single line to ground fault at phase A. The data from the external faults used to draw the new ellipses during the fault that happened at the beginning of the 3rd cycle of the simulation near the high voltage side. The ellipse deformation triggered the detection criterion as shown at Fig. (11) to (12). The values k_0, $\Delta i_{n\ at\ H.V}$ and $\Delta i_{n\ at\ L.V}$ of each cycle of the simulated data were calculated at Table V as shown below. The results showed that the values of k_{0diff} of 0.01367744 and 0.01121428 at phase A have bypassed the threshold value of 0.00011074, Therefore $\Delta i_{n\ at\ H.V}$ and $\Delta i_{n\ at\ L.V}$ were calculated after 16 sample of fault occurrence. The values of the faulted phase A $\Delta i_{n\ at\ H.V}$ = -0.01845 and $\Delta i_{n\ at\ L.V}$ =-0.01991 have the same polarity during external fault. The same polarity confirms that the detected fault is external fault.

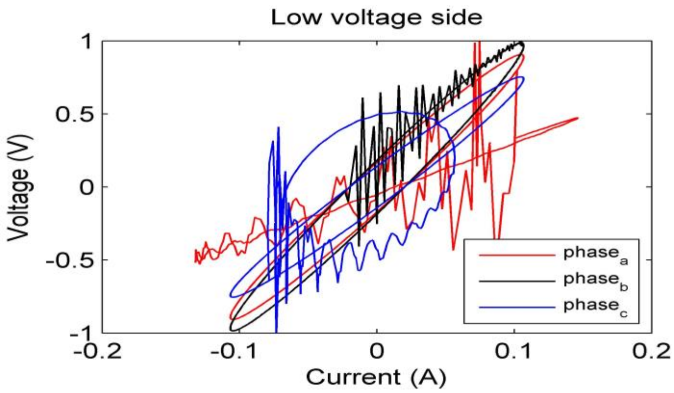

Fig. 11. Ellipse at the low voltage side of the transformer at external fault case with 90^0 fault inception angle

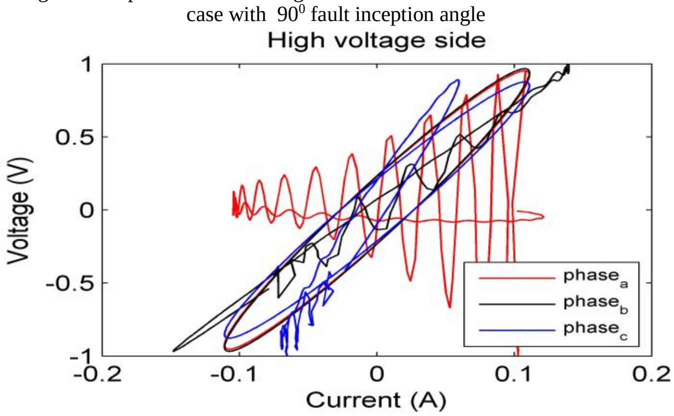

Fig. 12. Ellipse at the high voltage side of the transformer at external fault case with 90^0 fault inception angle.

TABLE V. THE CENTER VALUE DURING EXTERNAL FAULTED CYCLE AT PHASE A, $\Delta i_{n\ at\ H.V}$ AND $\Delta i_{n\ at\ L.V}$ AFTER 1/16 CYCLE.

	Phase A	Phase B	Phase C
k_{0diff} at H.V	0.01367744	0.00691213	0.00686751
k_{0diff} at L.V	0.01121428	0.00133591	0.00557622
$\Delta i_{n\ at\ H.V}$ at 90^0	-0.01845	0.013438	0.01344
$\Delta i_{n\ at\ L.V}$ at 90^0	-0.01991	0.000577	0.020773
$\Delta i_{n\ at\ H.V}$ at 36^0	-0.0001581	0.0007906	0.0007906
$\Delta i_{n\ at\ L.V}$ at 36^0	-0.001731	0	0.0014426
$\Delta i_{n\ at\ H.V}$ at 0^0	0.0173932	-0.007906	-0.007906
$\Delta i_{n\ at\ L.V}$ at 0^0	0.010675	-0.000404	-0.011541

C. Internal Fault Case

Phase to ground internal fault was applied at various parts of the transformer windings. Two data samples at 20 and 80 percent of the winding were presented at this case study. Moreover the fault was calculated at different inception angles. A shape of a deformed ellipse can be seen as in Fig. (13) to (17) respectively at the internal fault cases that will trigger the detection criterion.

After capturing the values of the centers at the different cases of internal fault. k_{0diff}, $\Delta i_{n\ at\ H.V}$ and $\Delta i_{n\ at\ L.V}$ for the 20 and 80 percentage winding fault were calculated. The high values of k_{0diff} 0.0108107, 0.0004518, 0.07365468, 0.00480387 for 20 and 80 percent fault respectively will trigger the fault detection criterion. $\Delta i_{n\ at\ H.V}$ and $\Delta i_{n\ at\ L.V}$ are measured after 16 sample (1/16 cycle) of the detection as shown in Table VI and Table VII respectively.

The values of $\Delta i_{n\ at\ H.V}$ and $\Delta i_{n\ at\ L.V}$ at 20% fault were 0.074053 and -0.00087 while at 80% were 0.5281203 and -0.013849. Thus, it was concluded that the polarities of $\Delta i_{n\ at\ H.V}$ and $\Delta i_{n\ at\ L.V}$ are always opposite in all of the internal fault cases as shown in tables VI and VII. This mean that, the relay will be able to discriminate between internal and external faults.

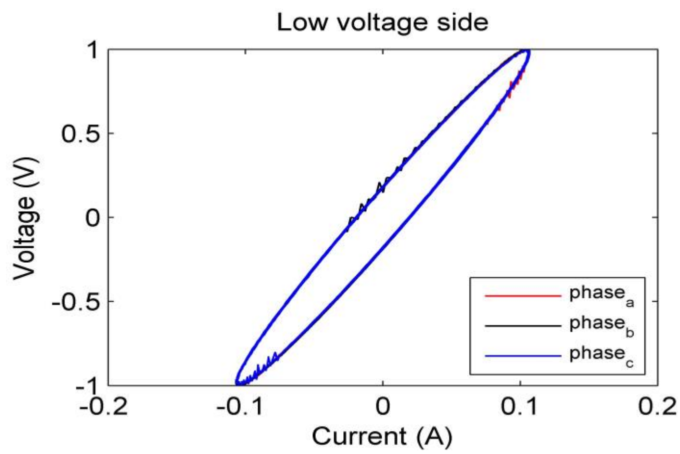

Fig. 13. Ellipse at the low voltage side of the transformer at 20% internal fault case with 90^0 fault inception angle

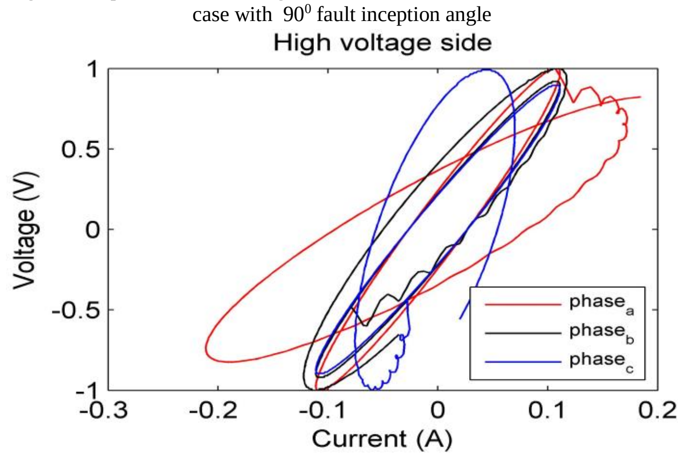

Fig. 14. Ellipse at the high voltage side of the transformer at 20% internal fault case with 90^0 fault inception angle.

ISBN: 978-988-14048-6-2
ISSN: 2078-0958 (Print); ISSN: 2078-0966 (Online)

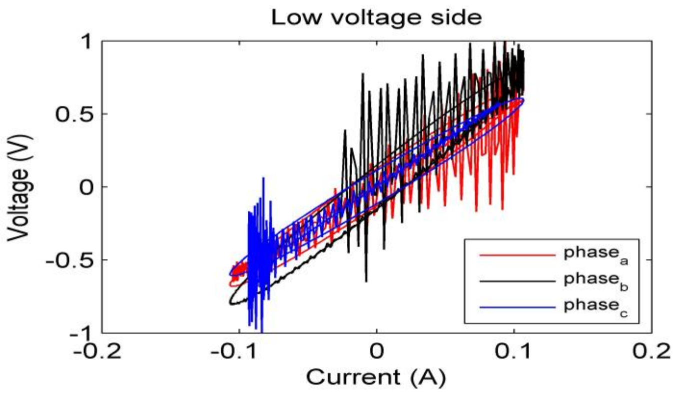

Fig. 15. Ellipse at the low voltage side of the transformer at 80% internal fault case with 90^0 fault inception angle.

.

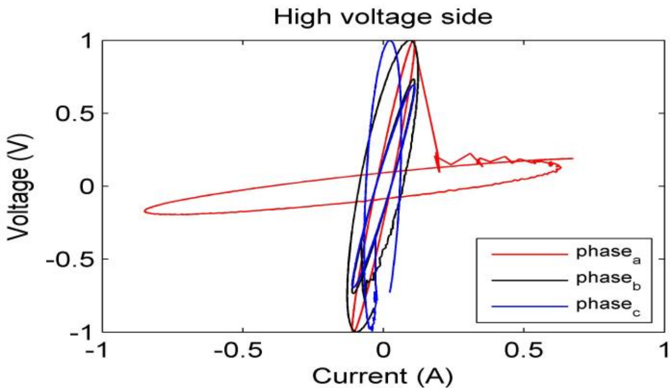

Fig. 16. Ellipse at the high voltage side of the transformer at 80% internal fault case with 90^0 fault inception angle.

TABLE VI. THE CENTER VALUE DURING INTERNAL FAULTED CYCLE AT 20% WINDING OF PHASE A, $\Delta i_{n\,at\,H.V}$ AND $\Delta i_{n\,at\,L.V}$ AFTER 1/16 CYCLE.

	Phase A	Phase B	Phase C
k_{0diff} at H.V	0.0108107	0.0066823	0.0066922
k_{0diff} at L.V	0.0004518	0.0000133	0.000338
$\Delta i_{n\,at\,H.V}$ at 90^0	0.074053	0.043588	0.043483
$\Delta i_{n\,at\,L.V}$ at 90^0	-0.00087	0.000289	0.000866
$\Delta i_{n\,at\,H.V}$ at 36^0	0.0047963	0.0026353	0.0026353
$\Delta i_{n\,at\,L.V}$ at 36^0	-0.000289	0	0
$\Delta i_{n\,at\,H.V}$ at 0^0	-0.0466454	-0.0273811	-0.0271439
$\Delta i_{n\,at\,L.V}$ at 0^0	0.0002885	-0.0000577	-0.000577

TABLE VII. THE CENTER VALUE DURING INTERNAL FAULTED CYCLE AT 80% WINDING OF PHASE A, $\Delta i_{n\,at\,H.V}$ AND $\Delta i_{n\,at\,L.V}$ AFTER 1/16 CYCLE.

	Phase A	Phase B	Phase C
k_{0diff} at H.V	0.07365468	0.01105655	0.01065150
k_{0diff} at L.V	0.00480387	0.00008693	0.00422294
$\Delta i_{n\,at\,H.V}$ at 90^0	0.5281203	0.0516762	0.0516525
$\Delta i_{n\,at\,L.V}$ at 90^0	-0.013849	0.0002885	0.0144257
$\Delta i_{n\,at\,H.V}$ at 36^0	0.0493334	0.003953	0.003953
$\Delta i_{n\,at\,L.V}$ at 36^0	-0.001154	0	0.0008655
$\Delta i_{n\,at\,H.V}$ at 0^0	-0.3402212	-0.0339958	-0.0337322
$\Delta i_{n\,at\,L.V}$ at 0^0	0.0075014	-0.000462	-0.008367

IV. CONCLUSION

This paper presented a new Ellipse technique (ET) based algorithm for fault detection in high voltage power transformers. The suggested algorithm was successfully used to detect fault presence as well as discriminating between internal and external faults. Different fault cases have been simulated to verify this algorithm using ATP and Matlab. The obtained results showed great success of the proposed algorithm to discriminate between internal and external faults at different fault inception angles. The ET has the advantages of being fast simple and reliable. Further case studies, testing during inrush current and transients, and verifying this technique using a lab model is still under progress.

V. REFERENCES

[1] IEEE Power Engineering Society, *IEEE Guide for Protecting Power Transformers*, vol. 2008, no. May. 2008.

[2] J. L. Blackburn and T. J. Domin. Protective Relaying Principles and Applications. Boca Raton, USA: CRC Press, 3ª Ed., 2007.

[3] B. Jeyasurya and M.A. Rahman "A state-of-the-art review of transformer protection algorithms" 534 IEEE Transactions on Power Delivery, Vol. 3," vol. 3, no. 2, pp. 534–544, 1988.

[4] I. Brncic, Z. Gajic, and T. Einarsson, "Transformer Differential Protection Improved by Implementation of Negative-Sequence Currents," [Online]. Available: http://citeseerx.ist.psu.edu/viewdoc/download?doi=10.1.1.617.794&rep=rep1&type=pdf

[5] M. Tripathy, R. Maheshwari, and H. Verma, "Improved transformer protection using probabilistic neural network and power differential method," *Int. J. Eng. …*, vol. 2, no. 3, pp. 29–44, 2010.

[6] R. Umre and P. V. T. Barhate, "Power transformer protection using Clark ' s transformation and fuzzy logic .," *Int. J. Eng. Res. Appl.*, no. April, pp. 34–39, 2014. [Online]. Available: http://www.ijera.com/special_issue/ICIAC_April_2014/EE/V2/EE-1353439.pdf

[7] M. Ahmadipour and Z. Moravej, "A New Approach in Power Transformer Differential Protection," 2013, pp. 46–57. [Online]. Available: http://inpressco.com/wp-content/uploads/2013/01/Paper746-571.pdf

[8] J. P. Marques and A. Oliveira, "Algorithm using Discrete Wavelet Transform to Power Transformers Protection," no. 2, 2013.

[9] Z. Hao and W. Chen, "Novel Power Transformer Differential Protection Scheme Based on Improved Short-window Algorithm," no. 51277142, pp. 830–834, 2016

[10] A. Pradesh, "Wavelet Transform and ANN base Differential Protection for Power Transformer," pp. 1882–1887, 2016.

[11] S. H. Haggag and A. M. El-rifaie, "A novel measurement technique for extra high voltage bus bar fault detection," no. 3, pp. 3–6, 2012.

[12] A. M. El-rifaie and R. M. Sharkawy, "A Practical Study For a New Measuring Tool For EHV Bus Bar Fault Detection," *Int. J. Eng. Appl. Sci.*, vol. 2, no. 6, pp. 0–4, 2015.

[13] S. H. Haggag, A. M. El-rifaie, and H. M. A. Mageed, "A New Fault Detection Tool for Single Phasing of a Three Phase Induction Motor," in *Proceedings of the World Congress on Engineering*, 2013, vol. II, pp. 3–7.

[14] S. M. Moussa and A. M El-rifaie, "Practical Application of the New Ellipse Measuring Technique for EHV Transmission Lines Protection," in *ElectrIMACS*, 2014, pp. 172–178.

[15] P. Bastard, P. Bertrand, and M. Meunier, "A Transformer model for winding fault studies," IEEE Trans. Power Delivery, vol. 9, no. 2, pp. 690-699, Apr. 1994.

ISBN: 978-988-14048-6-2
ISSN: 2078-0958 (Print); ISSN: 2078-0966 (Online)